OPEN ACCESS

University of BRISTOL

Link to published version (if available):
10.1109/TMTT.2010.2049679

Link to publication record in Explore Bristol Research
PDF-document

University of Bristol - Explore Bristol Research

General rights

Amplitude Offset Estimation by Phase Comparison in Suppression Loops

Paul A. Warr and Nirmal Bissonauth

Abstract—In this paper, a new architecture for an RF amplitude comparator circuit is introduced. The technique employs a trigonometric relationship enacted by passive RF components to map the amplitude ratio between two co-spectral RF signals into a phase difference. The theory of operation of the circuit is discussed in detail and the results of a practical investigation are presented, validating the approach. The results demonstrate an accuracy advantage over commercially available products. Over the frequency range of 1600–2100 MHz, amplitude offset measurements to within 0.08 dB of that of a calibrated vector signal analyzer are shown.

Index Terms—Amplitude estimation, measurement errors, phase measurement.

I. INTRODUCTION

THE APPROACH to amplitude offset estimation presented in this paper will find application in circuits where two signals are brought together in antiphase in order to suppress the output. This function is common in analog linearization circuits such as feedforward [1] and inherent error signal cancellation [2]. The system is not suitable for use as a general amplitude measurement instrument or as an offset measurement device if the amplitudes are arbitrary. Conventionally in suppression applications, a pilot tone (or spread spectrum pilot) is injected into the network and the residual presence of this signal is detected to attain information on the amplitude and phase balance of the suppression function. There are a number of shortcomings of this approach including the following.

- As suppression increases, the residual signal decays toward the noise floor and becomes difficult to detect.
- The amplitude of the residual signal does not provide enough information to resolve the phase and amplitude balance in the circuit, and thus, iteration of the balance control elements is required in order to maintain the suppression function.
- The phase variation of the residual signal becomes erratic as its amplitude approaches the system limit, and thus, cannot be used as a control metric.

The technique presented here overcomes these issues by sampling the two signals as they enter the combination stage and making comparative amplitude and phase measurements of them. The accuracy of available amplitude measurement hardware (e.g., 3%, if the absolute input power is selected carefully [3]) is insufficient for this purpose in a circuit where greater than 40 dB of suppression is desired, requiring an amplitude accuracy around 0.8% and phase accuracy around 0.5°. An absolute power measurement is not required for this application; only the difference in power between two signals is important. The solution presented here aims to measure this difference in an accurate manner by taking only phase measurements. As the two signals are in near-antiphase, available single-chip phase measurement hardware [3] is inaccurate. Thus, the technique includes stages to convert the signals to a near-quadrature relationship, at which point the phase measurement is at its most accurate. An increase in accuracy over standard power detection is attained by using phase measurement hardware at this optimum accuracy point.

The technique has advantages over previous systems for aligning amplitude and phase in suppression loops [4], [5] in that a pilot tone is not required, indeed the information-bearing signal may be used as the driving signal for the measurement process.

The estimation system merely samples the signals, and thus, its input amplitude may be controlled arbitrarily. High-impedance transistor gate/base nodes placed in parallel with the input port (e.g., 50 Ω) of the signal suppression entity is appropriate. The technique is suitable for realization on a RF integrated circuit (RFIC) for high-frequency broadband operation or, if only narrowband and/or low frequency operation is required, on a mixed signal application-specific integrated circuit (ASIC) (e.g., implemented in CMOS) where the addition of a closed-loop control system for amplitude and phase control may be envisaged on a single die.

This paper begins with a mathematical analysis of the circuit in order to demonstrate how an estimate of amplitude offset may be derived from a phase measurement. The technique is then validated via a practical investigation and results are presented. The results are analyzed and compared to those produced with a calibrated vector network analyzer (VNA) over the frequency range of 1600–2100 MHz.

II. THEORY OF OPERATION

The operation of the system is best explained through an analysis of the block diagram shown in Fig. 1.

The inputs to the system are the signals v_{in1} and v_{in2}. These signals are assumed to be co-spectral, in near-antiphase, and of near-equal power, as would be the case if one was used to suppress the other. Primarily, these inputs drive the suppression coupler, the output of which v_o is a function of the amplitude and antiphase offsets between the signals. v_{in1} and v_{in2}
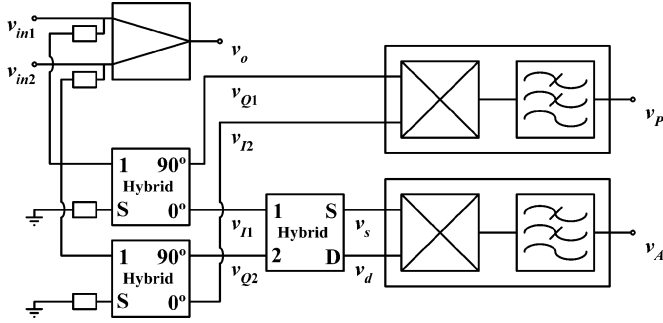
Fig. 1. Proposed circuit for phase and amplitude monitoring.

are sampled by resistive taps at the input to the suppression coupler. These taps have a resistance of at least an order of magnitude greater than the line impedance so that no degradation to the input power match of the circuit is observed. The sampled signals are passed to the amplitude and antiphase-offset measurement circuits; which ultimately output v_P, the phase offset metric, and v_A, the amplitude offset metric. The resistive taps may include shunt resistances in order to match the characteristic impedances of the hybrids; alternatively they be replaced with matched directional couplers or high input impedance active circuits.

A. Amplitude Comparator

Taking a continuous wave signal as an illustration of circuit operation, the inputs to the system may be defined as

$$v_{\text{in1}} = A_1 \cos(\omega t) \tag{1}$$

$$v_{\text{in2}} = -kA_1 \cos(\omega t + \phi) \tag{2}$$

where A_1 is the amplitude of the arbitrary reference signal, k is the scaling factor of the antiphase signal, and ϕ is the phase error of the antiphase relationship between the two signals [indicated by the minus sign present in (2)]. ϕ and k are expected to be small (less than $0 \pm 4°$ and 1 ± 0.02, respectively).

The amplitude comparator comprises a pair of 90° hybrid circuits driving a 180° hybrid circuit; the output of which drives a mixer-based phase comparator. It is shown below that the phase difference between the two signals v_s and v_d exiting the 180° hybrid circuit, given by v_A, provides the estimate for the amplitude ratio k of the two input signals v_{in1} and v_{in2}.

The 90° hybrid phase shifts one of the signals to form v_{Q2}, and this is passed to the 180° hybrid. The second 90° hybrid ensures that equivalent group delay is also present on v_{I1}. As the delay is balanced, the analysis can be simplified by omitting the common mode phase response of the circuit. Thus, at the input to the 180° hybrid,

$$v_{I1} = A_1 \cos(\omega t) \tag{3}$$

$$v_{Q2} = -kA_1 \cos\left(\omega t + \phi - \frac{\pi}{2}\right)$$

$$= -kA_1 \sin(\omega t + \phi). \tag{4}$$

The output produced by the 180° hybrid circuit comprises a sum v_s, and difference v_d signals defined as follows:

$$
\begin{aligned}
v_s &= v_{I1} + v_{Q2} \\
&= A_1 \cos(\omega t) - kA_1 \sin(\omega t + \phi) \\
&= A_1 \cos(\omega t) - kA_1 [\sin(\omega t)\cos(\phi) + \cos(\omega t)\sin(\phi)] \\
&= [A_1 - kA_1 \sin(\phi)]\cos(\omega t) - kA_1 \cos(\phi)\sin(\omega t) \quad (5)
\end{aligned}
$$

$$
\begin{aligned}
v_d &= v_{I1} - v_{Q2} \\
&= A_1 \cos(\omega t) + kA_1 \sin(\omega t + \phi) \\
&= A_1 \cos(\omega t) + kA_1 [\sin(\omega t)\cos(\phi) + \cos(\omega t)\sin(\phi)] \\
&= [A_1 + kA_1 \sin(\phi)]\cos(\omega t) + kA_1 \cos(\phi)\sin(\omega t). \quad (6)
\end{aligned}
$$

The phase relationship between v_s and v_d is shown below to be a function of the amplitude ratio k between the input signals v_{in1} and v_{in2}. v_s and v_d are first expressed in their respective (not root mean square (rms) scaled) phasor forms $\bar{V}_s$ and $\bar{V}_d$.

From (5),

$$\bar{V}_s = \begin{pmatrix} A_1 - kA_1 \sin(\phi) \\ -kA_1 \cos(\phi) \end{pmatrix}. \tag{7}$$

From (6),

$$\bar{V}_d = \begin{pmatrix} A_1 + kA_1 \sin(\phi) \\ kA_1 \cos(\phi) \end{pmatrix}. \tag{8}$$

The dot product is used to determine the phase angle θ between the two signals. Thus,

$$
\begin{aligned}
\bar{V}_s \cdot \bar{V}_d \\
&= [A_1 - kA_1 \sin(\phi)][A_1 + kA_1 \sin(\phi)] \\
&\quad + [-kA_1 \cos(\phi)][kA_1 \cos(\phi)] \\
&= A_1^2 - k^2 A_1^2 \sin^2(\phi) - k^2 A_1^2 \cos^2(\phi) \\
&= A_1^2 - k^2 A_1^2 \quad (9)
\end{aligned}
$$

$$
\begin{aligned}
|\bar{V}_s| \\
&= \sqrt{[A_1 - kA_1 \sin(\phi)]^2 + [-kA_1 \cos(\phi)]^2} \\
&= \sqrt{A_1^2 - 2kA_1^2 \sin(\phi) + k^2 A_1^2 \sin^2(\phi) + k^2 A_1^2 \cos^2(\phi)} \\
&= \sqrt{A_1^2 - 2kA_1^2 \sin(\phi) + k^2 A_1^2} \quad (10)
\end{aligned}
$$

$$
\begin{aligned}
|\bar{V}_d| \\
&= \sqrt{[A_1 + kA_1 \sin(\phi)]^2 + [kA_1 \cos(\phi)]^2} \\
&= \sqrt{A_1^2 + 2kA_1^2 \sin(\phi) + k^2 A_1^2 \sin^2(\phi) + k^2 A_1^2 \cos^2(\phi)} \\
&= \sqrt{A_1^2 + 2kA_1^2 \sin(\phi) + k^2 A_1^2} \quad (11)
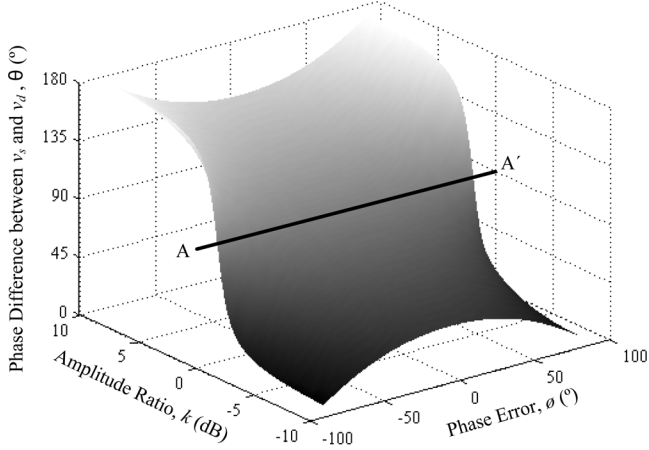\end{aligned}
$$

Fig. 2. Phase difference θ between V_s and V_d against amplitude ratio k and phase error ϕ. The dependency of θ on ϕ is at a minimum along the line A–A'.

Fig. 3. Error in measuring the amplitude ratio k when phase error ϕ is assumed to be zero for varying actual phase error and observed phase difference θ. Amplitude estimate error reduces to zero on the lines A–A' and B–B'.

$$\cos(\theta)$$

$$= \frac{\bar{V}_s \cdot \bar{V}_d}{|\bar{V}_s| \cdot |\bar{V}_d|}$$

$$= \frac{A_1^2 - k^2 A_1^2}{\sqrt{A_1^2 - 2kA_1^2 \sin(\phi) + k^2 A_1^2}\sqrt{A_1^2 + 2kA_1^2 \sin(\phi) + k^2 A_1^2}}$$

$$= \frac{1 - k^2}{\sqrt{1 - 2k\sin(\phi) + k^2}\sqrt{1 + 2k\sin(\phi) + k^2}}$$

$$= \frac{1 - k^2}{\sqrt{1 + 2k^2[1 - 2\sin^2(\phi)] + k^4}}$$

$$= \frac{1 - k^2}{\sqrt{1 + 2k^2 \cos(2\phi) + k^4}}. \tag{12}$$

Equation (12) shows the relation between the phase difference θ, amplitude ratio k, and phase error ϕ. A surface plot of θ against k and ϕ is shown in Fig. 2. The figure shows that, as $k \to 1$ (0 dB), the dependency of θ on ϕ reaches a minimum (along the line A–A' in Fig. 2). Thus, the two system aims of amplitude and antiphase balance may be simultaneously met. From this result, it may be assumed that phase error ϕ is not critical in determining the amplitude ratio k. When $k \to 1$ (0 dB), the value of θ is also near $90°$; when the phase detector is operating with greatest accuracy.

Of importance to this application is the relation between k and θ in the region where $\phi \to 0$ and $k \to 1$. In this region, the error in the measurement of k is found to be very small. This error is shown in Fig. 3 for varying actual phase error ϕ and varying observed phase difference θ in the region $\phi \to 0$ and $k \to 1$. This figure shows that, as $\theta \to 90°$, the error in the measurement of k reduces to zero regardless of the phase error ϕ. On Fig. 4, the lines A–A' and B–B' indicate zero systematic error in the amplitude estimate. Thus, a system that aims to drive the amplitude difference between two near-antiphase signals to zero, based on this measurement technique, does not require knowledge of the finite phase error.

Therefore, ϕ may be assumed to be zero for the amplitude measurement and (12) may be simplified and rearranged to give
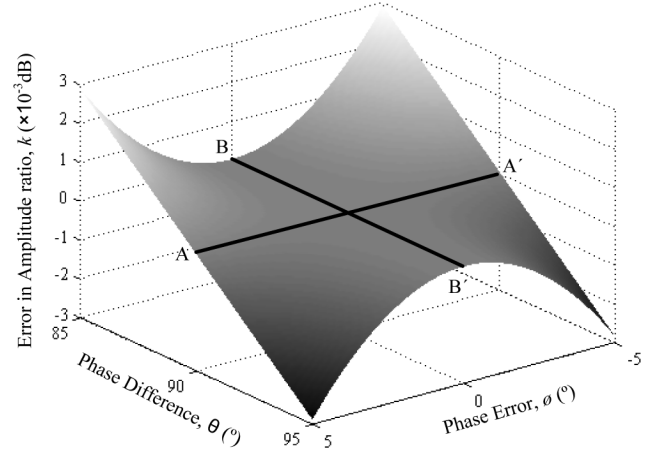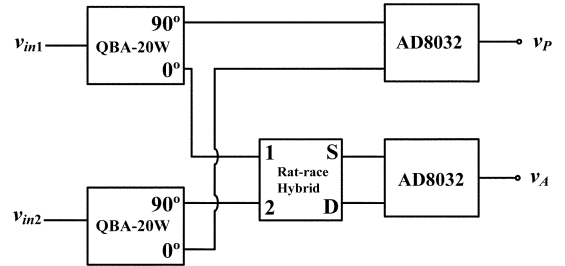

Fig. 4. Hardware demonstrator schematic: v_P is the phase comparison output voltage, which relates to $\angle(v_{in2}) - \angle(v_{in1})$ and v_A is the amplitude comparison output voltage which relates to $|v_{in2}|/|v_{in1}|$.

$\theta = f(k)$ in the region where $\theta \to 90°$. Thus,

$$\theta = \cos^{-1}\left(\frac{1 - k^2}{1 + k^2}\right). \tag{13}$$

By the application of the chain and quotient rules for differentiation, it can be shown that the rate of change of θ with k is given by

$$\frac{d\theta}{dk} = \frac{-1}{\sqrt{1 - \left(\frac{1-k^2}{1+k^2}\right)^2}} \cdot \frac{-4k}{(1 + k^2)^2} \tag{14}$$

which may be simplified to

$$\frac{d\theta}{dk} = \frac{2}{1 + k^2}. \tag{15}$$

Thus, for $k \to 1$ (0 dB), (15) shows that the rate of change of phase difference between the two signals entering the phase comparison process is 1 rad/unit-k (2 rad/dB). Fig. 2 shows that this rate is at a maximum. Therefore, if a phase comparison could be made between these two signals with greater than half the accuracy in absolute radians than could be observed on the difference in power of the two, then a more accurate amplitude estimation would result. This is the basis of the technique reported here.

Best case commercial amplitude comparators offer accuracy of ± 1 dB (± 0.12 amplitude factor) for near-equal amplitude signals up to 2.2 GHz over the commercial temperature range [3]. Lower accuracy is attained if individual amplitude measurement components are used [6]. However, under the same conditions, commercial phase comparators offer accuracy of $\pm 2°$ if the signals entering the comparator are in near-quadrature [3].

This technique exploits the increased accuracy of phase comparison techniques operating on input signals in near-quadrature to provide an amplitude offset estimation of significantly greater accuracy than that available by direct measurement.

Equation (15) shows that, as k diverges from 0 dB (in either direction) the variation of θ with k decreases. If the offset is 1 dB in either direction, the rate of change of k falls to 1 rad/dB. If the offset is 2 dB, the rate of change of k falls to 0.4 rad/dB.

B. Phase Comparator

The phase comparator is driven via a pair of $90°$ hybrid circuits, one input being taken from the $90°$ port of one hybrid and the other from the $0°$ port of the second hybrid. A phase comparator normally comprises a mixer circuit followed by a low-pass filter. For small phase errors $\phi \to 0$, phase discrimination can be maximized by this introduction of a $90°$ phase shift to one of the inputs. In Fig. 1, v_{Q1}, the input to the mixer element of the phase comparator, is phase-shifted. The other input is also passed through a $90°$ hybrid, but the nonphase-shifted output is selected, v_{I2}. This ensures that the group delay introduced by the $90°$ hybrid circuit is present on both inputs to the phase comparator.

Assuming the same inputs to the system as given in (1) and (2),

$$v_{I2} = -kA_1\cos(\omega t + \phi) \quad (16)$$

$$v_{Q1} = A_1\cos(\omega t - \pi/2) = A_1\sin(\omega t). \quad (17)$$

The output of the mixer v_{m1} can be written as the product of v_{Q1} and v_{I2} and simplified into a sum of the two constituent sine functions to give

$$v_{m1} = \frac{kA_1^2}{2}[\sin(\phi) - \sin(2\omega t + \phi)]. \quad (18)$$

Low-pass filtering the mixer output v_{m1} produces the signal v_p, which is a sine function of the phase difference ϕ

$$v_p = \frac{kA_1^2}{2}\sin(\phi). \quad (19)$$

This signal has a rate of change $\delta v_p/\delta\phi$, which is given by

$$\frac{\delta v_p}{\delta\phi} = \frac{kA_1^2}{2}\cos(\phi) \quad (20)$$

which is at a maximum when $\phi \to n\pi, n = 0, 1, 2, \ldots$.

Thus, as $\phi \to 0$ in this application, the accuracy of the phase measurement is maximized.

III. RESULTS

A hardware demonstrator was built based on Fig. 1 in order to validate this analysis and is shown in Fig. 4.

The $90°$ hybrids are Mini-Circuits QBA-20 W [7] and the phase comparators are Analog Devices AD8302 [6]. The rat-

race hybrids is realized in microstrip on a GIL Technologies MC5 high-frequency laminate (0.03 in). The bandwidth over which this demonstrator operates is defined by that of the $90°$ hybrids, i.e., 1600–2200 MHz.

A signal generator provides the test signal, which is split into two antiphase signals, substantially of equal power. Elements are placed in the two signal paths in order to control their amplitude and phase relationship around the antiphase and equal-power point. The difference between the two channel elements produces the small error in amplitude and phase that the comparator circuits measure. The $0°$ output is connected to the Channel A element, while the $180°$ output is connected to the Channel B element. These are, in turn, connected to the $v_{\mathrm{in}1}$ and $v_{\mathrm{in}2}$ inputs of the amplitude and phase measurement circuit. In the case of this prototype circuit, the inputs directly drive the $90°$ hybrids, rather than driving the suppression combiner and being sampled by resistive taps, as depicted in Fig. 1.

The differences between the pairs of channel elements were also measured by a through, open, short, and match (TOSM)-calibrated VNA to give a "best practical case" by which the performance of the technique could be assessed. There is some residual unmeasured error between the VNA benchmark and that observed by the technique due to the re-mating transfer response accuracy of the connectors [8].

A reference measurement is required to remove gain and phase errors present between the two channels of the comparator circuits before any comparative tests can be performed. These errors arise from issues such as amplitude imbalance and phase errors in the $90°$ hybrid circuits and within the AD8302 phase comparators. For the reference measurement, elements were inserted into Channels A and B, and the output of the amplitude and phase measurement circuits were noted. All performance measurements were made by replacing one of the reference elements and the change in output of the circuit was noted. This may be considered as a calibration step to account for fixed systematic offsets. The assumption of consistency is valid for measurements near the operating point defined by $\phi \to 0$ and $k \to 1$.

The input frequency was varied from 1600 to 2100 MHz and the differences in amplitude and phase were recorded against frequency. The results from the tests demonstrate the accuracy of the phase and amplitude measurement circuits.

A. Phase Measurement

The results here benchmark the accuracy of the phase measurement, and therefore, the utilization of the AD8302 devices: a "best case" expectation of the amplitude accuracy is established. This device also had an amplitude measurement function that is used as a benchmark for the performance available from amplitude measurement devices based on logarithmic amplifiers.

Four elements were measured with phase delays up to $8°$ (mid band).

Fig. 5 shows the phase difference effected by the delay elements across the range of 1600–2100 MHz measured by the phase comparator circuit. Also shown is the result of the independent VNA phase measurement of the elements relative to the systematic offset calibration.
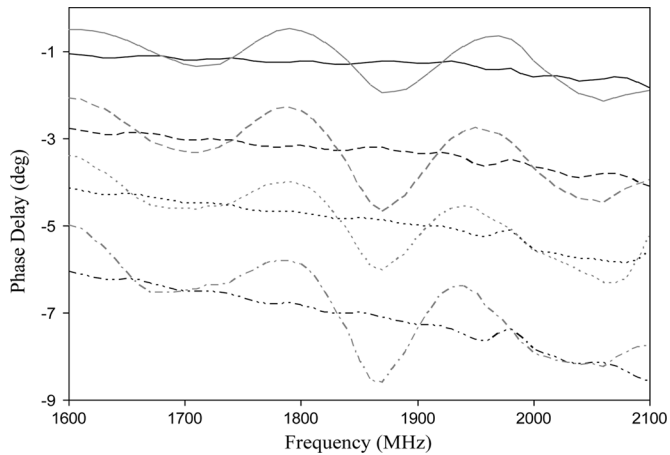
Fig. 5. Characteristic of delay elements using VNA and the phase comparator circuit. The hatching pattern of the traces identifies the pairs of VNA and measured data. Each pair comprises one dark trace (VNA data) and one light trace (measured data).
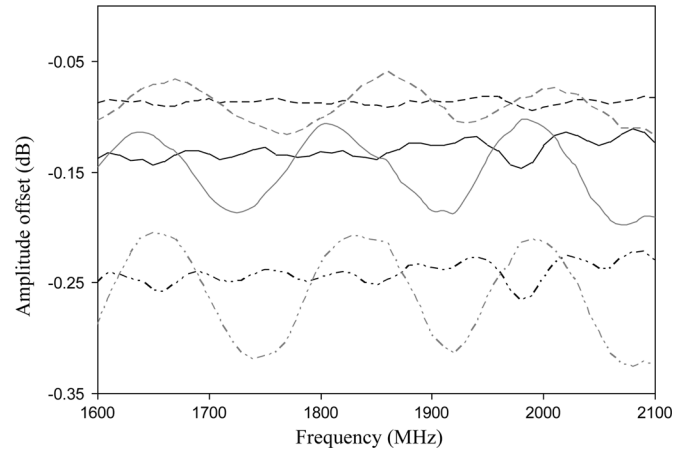

Fig. 6. Comparison of attenuator elements using amplitude comparator circuit and VNA. The hatching pattern of the traces identifies the pairs of VNA and measured data. Each pair comprises one dark trace (VNA data) and one light trace (measured data).

The required instrumentation to interpret the amplitude offset estimation output of the system is the same as that required for the phase offset, as both are provided by phase-voltage output of instances of the same device (in this case, AD8302). The phase-voltage output is within the range of 0–1.8 V and may be directly observed by an instrument drawing less than 8 mA or sampled for digital processing.

The phase output from the AD8302 circuit limits the performance of both the phase and amplitude comparator circuits. From the plots of the phase difference against frequency in Fig. 5, it is seen that the observed phase difference can vary by as much as $\pm 1.5°$ from the VNA measurement.

B. Amplitude Measurement

The reference measurement for this test followed the same form as the phase measurements. The tests were performed by replacing the Channel B attenuator element with three test attenuator elements.

Fig. 6 shows the amplitude difference effected by the test elements across the range of 1600–2100 MHz, measured by the amplitude comparator circuit. Also shown is the result of the independent VNA phase measurement of the elements relative to the systematic offset calibration.

Fig. 6 shows that the practical application of this technique for measuring amplitude offsets offers a measurement tolerance of ± 0.08 dB over a broad band (with respect to a calibrated VNA measurement). This compares favorably with the amplitude measurement tolerance offered by commercial devices (e.g., AD8032), which typically quote ± 1-dB linearity. The increased accuracy of this technique may be attributed to the use of phase comparison at its most accurate operational point and the high rate of change of phase with respect to amplitude offset in this region.

The cyclic nature of the phase and amplitude offset error in the frequency domain is indicative of mismatch between transmission line and source/load ports. It is likely that greater accuracy will result if these mismatches are removed, although this is not included in the current investigation.

The frequency-domain period of the cycles in the output accuracy correlates with the electrical length of the matched cables used in the prototype circuit. The proven system accuracy of gain and phase measurement approaches that of the re-mating transfer response accuracy of the subminiature A (SMA) connectors used in the test elements and throughout the prototype circuit [8]. Therefore, further attempts to increase the system performance with respect to the VNA-measurement benchmark would not be valid with this discrete implementation.

IV. CONCLUSION

The accuracy of the phase measurement circuit with respect to a VNA measurement was found to be $\pm 1.5°$ over the measured frequency range as expected from the quoted accuracy in the phase comparator data sheet. Tests performed with attenuator elements showed that the amplitude comparator circuit could measure differences with an accuracy of ± 0.08 dB with respect to a VNA measurement. The method is a valid means of measuring amplitude differences offering greater accuracy than that of commercial products. The derivation of an amplitude offset metric from a phase measurement made at the optimum relationship between inputs facilitates this additional accuracy.

When used in a suppression loop system, this approach offers significant advantages over traditional methods as a pilot tone (or spread-spectrum equivalent) is not employed.

Implementation in integrated form as either an RFIC or mixed signal ASIC is likely to yield increased accuracy by removing mismatch-based errors in the system. Design-time efficiency is inherent in this approach as sub-circuit reuse is prevalent across the architecture.

REFERENCES

[1] P. B. Kenington, R. J. Wilkinson, and J. D. Marvill, "The design of highly linear broadband power amplifiers," *IEE Solid-State Power Amplifiers Colloq.*, pp. 5/1–5/4, Dec. 16, 1991.

[2] P. A. Warr, M. A. Beach, and J. P. McGeehan, "Amplifier linearisation by exploitation of backwards-travelling signals," *Electron. Lett.*, vol. 38, no. 6, pp. 260–261, Mar. 2002.

[3] "Analog Devices AD8313," Analog Devices, Norwood, MA, Data Sheet, Jun. 2004. [Online]. Available: http://www.analog.com/

[4] S. Kang, U. Park, K. Lee, and S. Hong, "Adaptive feedforward amplifier using pilot signal," in *10th Int. Telecommun. Conf.*, Feb 23–Mar. 1, 2003, vol. 1, pp. 677–680.

[5] G. T. Watkins and P. A. Warr, "Flexible linearity profile low noise feedforward amplifiers for improving channel capacity," in *57th IEEE Semiannu. Veh. Technol. Conf.*, Apr. 22–25, 2003, vol. 3, pp. 1567–1570.

[6] "Analog Devices AD8302," Analog Devices, Norwood, MA, Data Sheet, Jul. 2002. [Online]. Available: http://www.analog.com/

[7] "QBA-20W, surface mount splitter/combiner," Mini-Circuits, Brooklyn, NY. [Online]. Available: http://www.minicircuits.com/QBA-20W.pdf, (last accessed August 21, 2005)

[8] J. R. Juroshek, "A study of measurements of connector repeatability using highly reflecting loads," *IEEE Trans. Microw. Theory Tech.*, vol. MTT-35, no. 4, pp. 457–460, Apr. 1987.

Paul A. Warr received the B.Eng. degree in electronics and communications from The University of Bath, Bath, U.K., in 1994, and the M.Sc. degree in communications systems and signal processing and Ph.D. degree from The University of Bristol, Bristol, U.K., in 1996 and 2001, respectively. His doctoral research concerned octave-band linear receiver amplifiers.

He is currently a Senior Lecturer of electronics with The University of Bristol. His research concerns the front-end aspects of software (reconfigurable) radio and diversity-exploiting communication systems, responsive linear amplifiers, flexible filters, and linear frequency translation. His research has been funded by the U.K. Department of Trade and Industry (DTI)/Engineering and Physical Sciences Research Council (EPSRC) alongside European Framework programs and industrial collaborators.

Nirmal Bissonauth received the B.Sc. degree in electronics and computer science from Keele University, Stoke, U.K., in 1996, the M.Sc. degree in communications systems and signal processing from The University of Bristol, Bristol, U.K., in 2005, and is currently working toward the Ph.D. degree (part time) at The University of Bristol.

He is currently an Analog Design Engineer with Phyworks Ltd., Bristol, U.K., where he is involved with cable and backplane equalizer integrated circuits. His research concerns the investigation of techniques for linearizing mixers.